

Article

Exploring the Effect of Misinformation on Infectious Disease Transmission

Nabeela Mumtaz ^{1,*} , Caroline Green ²  and Jim Duggan ^{1,2,3} 

¹ School of Computer Science, National University of Ireland Galway, H91 TK33 Galway, Ireland; james.duggan@nuigalway.ie

² Data Science Institute, National University of Ireland Galway, H91 TK33 Galway, Ireland; caroline.green@nuigalway.ie

³ Ryan Institute, National University of Ireland Galway, H91 TK33 Galway, Ireland

* Correspondence: n.mumtaz1@nuigalway.ie

Abstract: Vaccines are one of the safest medical interventions in history and can protect against infectious diseases and ensure important health benefits. Despite these advantages, health professionals and policymakers face significant challenges in terms of vaccine rollout, as vaccine hesitancy is a global challenge, and varies greatly with context, i.e., place, time, and vaccines. The internet has rapidly become a widely used information source for health-related issues, and a medium where misinformation in relation to vaccines on social media can spread rapidly and influence many. This research models the impact of vaccine confidence on the transmission of infectious diseases. This involves two interacting contagion models, one for the disease itself, and the other for the public's views on vaccination. Sensitivity analysis and loop impact analysis are used to explore the effects of misinformation and vaccine confidence on the spread of infectious diseases. The analysis indicates that high vaccine confidence has a reinforcing effect on vaccination levels and helps to reduce the spread of an infectious disease. The results show that higher vaccine confidence can mitigate against the impact of misinformation, and by doing so can contribute to the enhanced control of an infectious disease outbreak.



Citation: Mumtaz, N.; Green, C.; Duggan, J. Exploring the Effect of Misinformation on Infectious Disease Transmission. *Systems* **2022**, *10*, 50. <https://doi.org/10.3390/systems10020050>

Academic Editor: Andreas Größler

Received: 17 March 2022

Accepted: 13 April 2022

Published: 15 April 2022

Publisher's Note: MDPI stays neutral with regard to jurisdictional claims in published maps and institutional affiliations.



Copyright: © 2022 by the authors. Licensee MDPI, Basel, Switzerland. This article is an open access article distributed under the terms and conditions of the Creative Commons Attribution (CC BY) license (<https://creativecommons.org/licenses/by/4.0/>).

Keywords: vaccine confidence; misinformation; infectious disease transmission; sensitivity analysis; loop impact analysis

1. Introduction

Vaccines are one of the safest and most effective medical interventions in history [1]. They are a key pharmaceutical intervention for controlling the spread of infectious diseases, which is an increasingly challenging task due to factors such as the ease of global travel [2]. Overall, there are a variety of vaccines in use, for example: (i) vaccines included in the vaccination calendar (for instance, influenza, flu, polio, etc.); (ii) vaccines against endemic diseases, including those used for travel (e.g., yellow fever); and (iii) vaccines against emerging viruses, most recently, for example, SARS-CoV-2. The positive impact of vaccine rollout can be demonstrated through the success of the World Health Organization initiative that eradicated smallpox through mass vaccination. It is also worth noting the number of commercially licensed vaccines used as countermeasures for infectious diseases, for example, in the USA there are of the order of 64 vaccine types listed for 26 different pathogens [3]. Despite these public health successes, vaccine deployments have always been challenged by individuals and groups who question, and sometimes refuse, vaccines for a variety of reasons, including religious, scientific, and political [4]. This lack of confidence, or hesitancy, is a complex, multi-faceted phenomenon that dates back to the immunisation performed by Dr Zabdiel Boylston (1721) and Edward Jenner (1796–1798) [5]. Vaccine hesitancy refers to “the delay in acceptance or refusal of vaccination despite the availability of vaccination services” [6], and as such, can have significant consequences

for public health, especially when it undermines herd immunity [7]. Heidi J. Larson [8], a professor of infectious disease epidemiology in the UK, in an interview, asserted that the vaccine-hesitant population portion is large enough to undermine efforts to achieve immunity and reduce hospitalisations.

Larson et al. [9] describe vaccine-hesitant individuals as a heterogeneous group who hold varying degrees of indecision about specific vaccines or vaccination in general. This is a global issue, as the WHO reports that the delay in acceptance or refusal of vaccines (despite the availability of vaccination services) has been reported in more than 90% of countries in the world [10]. In terms of underlying reasons for vaccine hesitancy, a number of studies have identified the following issues:

- Karafillakis and Larson [11] identified the most common reasons for vaccine hesitancy, namely, perceptions that: (1) new vaccines are developed too quickly resulting in insufficient testing; (2) a pandemic is not a life-threatening illness, and is comparable to mild flu; and (3) a vaccine could cause disease and long-term adverse reactions;
- Lorini et al. [7] summarised the '3C' model of factors for vaccine hesitancy. The factors that influence the vaccination decision are: (1) complacency, as people do not value the vaccine as a need, (2) convenience, in that the vaccine is difficult to access, and (3) confidence, as the vaccine or provider is not trusted;
- Wiyeh et al. [12] described the spread of vaccine hesitancy as an "outbreak". The researchers make a distinction between vaccine hesitancy behaviours: baseline vaccine hesitancy, which refers to the level of refusal or delay in vaccine acceptance that is constantly present in the population and, while it may vary, changes are unlikely to be sudden; reactive vaccine hesitancy, where the delay in acceptance due to vaccine-related events shows a rapid spike in hesitancy levels, usually subsiding at a slow rate.

Tafuri et al. [13] argue that vaccine hesitancy is closely connected with increasing Internet use and the new information and communication technologies (ICTs). For example, in Italy, 80% of parents use the Internet to search for vaccine-related information [5]. Davies et al. [14] reported in 2002 that, "Vaccination" was searched across seven of the most used search engines and 43% of the top 10 results across all platforms contained anti-vaccine content, which encouraged vaccine refusal or emphasised the dangers of vaccines. Social networks also play an important role in affecting the dynamics of health behaviours; however, identifying the main drivers of health-behaviour spread in social networks has been challenging [15]. Larson et al. [16] reported that France has one of the highest rates of vaccine hesitancy in the world, at around 45%. Lahouati et al. [17] (2019) conducted a search on YouTube in France using the keyword "vaccines", and reported that "of all videos, 120 (72.2%) were considered anti-vaccine and 46 (27.8%) were pro-vaccine videos". Wiyeh et al. [12] reported on two studies to measure levels of vaccine hesitancy in the Philippines, in 2015 and 2018, which showed that baseline vaccine hesitancy increased nearly 30% due to a 2017 scandal concerning a seasonal dengue fever disease vaccine. The WHO advised that due to anti-vaccination efforts on social media, vaccine-preventable diseases are expected to lead to thousands of deaths over the next decade [9]. Lahouati et al. [17] concluded that "health professionals should be aware of the widely disseminated vaccination misinformation available on the Internet".

Over the last 20 years, social media has facilitated the spread of anti-vaccination information and vaccine hesitancy has risen globally. More recently, vaccines for COVID-19 have become available, and the primary concern of the WHO, health experts, and governments is the potentially low public acceptance of the COVID-19 vaccines, often fuelled by conspiracy theories that spread on social media. Recent examples of hesitancy include reports of a refusal rate of up to 40% by frontline workers in Los Angeles County and 60% of care home workers in Ohio [18]. In New Zealand, the government's Ministry of Health surveys reported that "40% of the population are sceptical towards COVID-19 vaccines, about 10% of the population say they will "definitely not" take a vaccine, with a further 20% unlikely to take one, and 11% are unsure about taking one" [19]. The U.S. is struggling with comparatively low vaccination rates because of high vaccine hesitancy among certain

demographic groups, and a lack of access to vaccination and trustworthy information in remote areas. Lack of trust in the Government is also a factor in vaccine hesitancy [20]. Thaker and Subramanian [19] found that exposure to COVID-19 vaccine misinformation and vaccine hesitancy leads to a decline in vaccination intentions.

The diffusion of ideas or information spreading is perceived as analogous to the transmission of an infectious disease. Recently, Sontag et al. developed a model that merged epidemiological dynamics with information spread [21]. They described that “the surge in awareness, arising from fast spread of information in the trusting population, can reduce the peak of infection and lead to a larger population that remains uninfected by the end of the outbreak” [21]. Misinformation transmission, similar to the transmission of a disease, is well suited for modelling because information transmission from person to person is clearly defined via human links and activities [22]. The SIR model for acute infectious diseases is widely used in epidemiology [23], and mathematical modelling is a practical approach to understanding the spread of misinformation. A person “infected” with a rumour can “infect” a person susceptible to rumour, and the infected person can recover from the rumour after some time [24]. In this study, we explore the effect of people exposed to misinformation on the spread of epidemics. Furthermore, many other factors help to explain the spread of misinformation and infectious diseases, such as a constant underlying level of vaccine-hesitant behaviour.

This paper is organised as follows: Section 2 presents a literature review of information/fear/rumour spread, infectious disease, and vaccination models; Section 3 explains the sensitivity and loop impact analysis method, the misinformation/disease model’s formulation, differential equations, and the feedback loop’s structure; Section 4 describes the misinformation/disease model’s sensitivity analysis and the loop impact analysis experiment results; and Section 5 presents insights from the experiments and our conclusions.

2. Literature Review

2.1. Related Information, Fear and Rumour Spreading Dynamic Models

Related research encompasses models that explore the spread of information, fear, and rumour with different modelling approaches. Bettencourt et al. [25] illustrated dynamic models to predict the average behaviour of heterogeneous populations given the spread of ideas, with or without an incubation class, which shows people who have acquired the information but have not yet spread it to others. The research discussed details the sociological reasons for the spread of information and ideas in three different communities. Epstein et al. [26] used a dynamic model to show the interaction of two contagion processes: disease and fear of the disease. They explored the effect of an individual’s adaptive behaviour of social distancing and self-isolating based on fear. Li [27] presented a simple rumour spreading model that focused on reducing rumour spreaders, and suggested the addition of an adjustment policy that could slow down rumour spreading. Liu et al. [28] developed an SEIR rumour spreading model with a hesitating mechanism. They believed that when a person infected with a rumour contacts a person susceptible to rumour, the individual susceptible to the rumour first experiences an incubation period before becoming infected with the rumour. The incubation delay slows down the rumour spread process in social networks. They modified the model with a feedback mechanism to weaken the spread of rumours. Wiyeh et al. [12] presented a model to show the spread of vaccine hesitancy as an “outbreak”. The researchers critically reviewed vaccine hesitancy behaviours and made a distinction between “baseline” and “reactive” vaccine hesitancy. The research interpreted vaccine hesitancy behaviour or rumours as analogous to an infection of the mind. The dynamics of rumour spreading and vaccine hesitancy have different possible behaviours. Larson represents vaccine hesitancy behaviour with Kurt Lewin’s behaviour equation $B = f(PE)$, namely, “behaviour is a function of the person and their environment” [29].

2.2. Related Infectious Disease and Vaccination Dynamic Models

Our literature review highlighted several infectious disease models that include a structure for vaccination. Ehrhardt et al. [30] described vaccination as a preventive measure against infectious disease, but since vaccine protection may diminish, individuals become susceptible again over time. Raimundo et al. [31] developed a mathematical model with two susceptible compartments to describe the dynamics of reinfection after vaccination and recovery. They represented the probability of waning immunity over time. Hamami et al. [32] developed an epidemiological model to investigate certain vaccine-preventable diseases (measles, mumps, and rubella (MMR)), which can reemerge in highly vaccinated populations due to temporary protection or waning. They critically analysed the loss of immunity between two high peaks of an epidemic outbreak in a homogeneously mixed population. Leung et al. [33] presented a dynamic model containing two waning compartments for waning immunity after disease recovery and vaccination. The research estimated that an infectious disease pattern may change when vaccine-induced immunity differs from that of infection-acquired immunity. Nkamba et al. [34] used a dynamic model to show the spread of the infectious disease tuberculosis (TB). Their analysis indicates that vaccination could reduce the spread of TB, but it does not completely eradicate it when the effective contact rate is high and vaccine efficacy is average. Rabiou et al. [35] developed a model containing seven compartments. The research analysed infectious disease transmission where fractions of the population are vaccinated, quarantined, or treated individuals. These are preventive measures to control the spread of an infectious disease.

Our literature search also summarised useful existing models that explore the spread of information/fear/rumours and infectious diseases. Most researchers developed one model with several compartments, in which multiple processes were represented by a single structure: disease and fear [26], rumours and adjustment approaches [27], and vaccine waning and preventive measures [33,35]. However, to the best of our knowledge, existing research has not: (1) combined a model of vaccine misinformation spread with an infectious disease transmission model and (2) investigated sensitivity and loop impact analysis on the model's feedback structure and behaviour. This paper combines the two diffusion dynamics: the spread of misinformation and the spread of disease, each of which can have different reproduction numbers. The spread of misinformation and the spread of disease are two phenomena. The focus of this research is to develop a dynamic model by combining the two diffusion dynamics and analysing its structure, behaviour, and feedback loops. This is in line with the idea of a small powerful model, and Ghaffarzadegan et al. [36] writes that "although small models may omit some of the details behind causal links, variables can and must remain operational at a high level". They further added that small-size models can reveal the link between the feedback structure and behaviour more easily.

3. Material and Methods

3.1. System Dynamics Sensitivity Analysis Combined with Loop Impact Analysis

The system dynamics approach is recognised as a powerful method for understanding and addressing complex health issues [37]. In system dynamics, stocks, flows, and feedback loops are the basic structural elements within the system boundary, and behaviour is generated through the interaction of reinforcing and balancing feedback loops. These model elements are responsible for generating the behaviour of the system [38]. A feedback loop is a set of interconnections between variables, which forms a closed path from a variable back to itself. There are two types of feedback loops:

1. Positive feedback loop (reinforcing), a feedback loop is positive if a change in the source variable will cause the target to change in the same direction;
2. Negative feedback loop (balancing), a feedback loop is negative if a change in the source variable will cause the target to change in the opposite direction.

A feedback loop's polarity can be calculated by tracing an increase in a variable around a feedback loop and observing its direction of change. The feedback loop's dominant structure can be identified by analysing the most critical feedback loop's behaviour and

establishing a connection between them. Duggan and Oliva [39] explained that identifying the structural elements that are responsible for a particular behaviour is a challenging task in a complex multi-state model. For any system dynamics model, understanding structural dominance through model analysis is an essential prerequisite for guiding robust policy design, and some important definitions include:

- Dominant loop: A loop that is primarily responsible for model behaviour over some time interval is known as a dominant loop [40];
- Dominant structure: A model's dominant structure is a subset of the model's feedback structure, which is responsible for the model's particular behaviour;
- Point of inflection (POI): A point of inflection is a time of notable change in a model's behaviour. It is a point on the logistic curve where the loop reaches half of its maximum value.

Before the advent of loop dominance tools, approaches were designed to provide a better understanding of structural behaviour. In 1994, Peterson and Eberlein [41] presented, using the simulation software Vensim, a procedure that can perform automated validity tests and check for the model's adherence to the expected behaviours pattern. Ford [39] stated that "feedback loop dominance is a critical tool in explaining how structure drives behaviour. Current analytic tools for loop dominance analysis are tacit, not codified, unable to accurately identify dominant loops or inapplicable to most models". In 2005, Ford and Flynn [42] described an iterative method, based on correlation, to learn which of the many uncertain inputs to a system dynamics model stands out as most influential.

Forrester, in 1982, proposed the eigenvalue elasticity analysis (EEA) method in the system dynamics field. The EEA method examines both link and loop significance regarding the dynamic behaviour of the model. It identifies the relationship between the parameters and feedback loops [43]. The EEA method has some weaknesses [44]: It requires identifying all feedback loops and all links they pass through in the model. If the model is highly complex with many feedback loops, this procedure becomes prohibitively difficult, and it fails to relate the identified dominant structure to any selected variable of interest. A drawback of the EEA approach is its reliance on abstract mathematical constructs, such as eigenvalues, which can be challenging to interpret and apply [44].

Mojtahedzadeh 1997, has proposed the pathway participation metric (PPM) method to understand structure behaviour. In contrast to the EEA, PPM adopts a minimalist approach in that pathways between two state variables are considered the primary building blocks of the influential structure. Eventually, some combinations of pathways define the most influential system structure, which contains a single feedback loop, in determining the behaviour of a state variable at a given time interval [44]. In other words, the PPM approach determines the magnitude of the change in the net flow of the stock. The PPM method's key strength is its ability to directly associate model behaviour to structure; on the other hand, the PPM method has a weakness in that it does not identify the dominance of behaviour modes [45].

More recently, Schoenberg et al. presented the loops that matter (LTM) method to show a strong relationship between a model structure and behaviour, whereby this method is used to explore "which links and feedback loops are responsible for generating observed model behaviour" [46]. LTM performs a "formal assessment of dominant structure and behaviour" for models of any size, complexity, or dimensionality" [47]. The LTM method is derived from PPM/loop impact apart from its treatment of link polarity. However, LTM is distinct in its application, measuring loop dominance across the entire model [48]. The LTM method includes causal pathways between stocks through all intermediate variables and performs all calculations directly on the original model equations. In this research, we deploy this newly developed LTM analysis approach.

The LTM method's strengths are: (1) it relates to the entire model; (2) it provides the link's scores, relative loop's scores, and the average relative loop scores; (3) it simplifies multiple feedback loops to highlight the most critical or dominant structure; (4) it indicates a point of inflection (POI) between the feedback loops; (5) the LTM can be combined with

sensitivity analysis to examine how independent variables impact on a particular loop behaviour; (6) it animates results, which is a useful aspect; and (7) it is generally applicable to all models. The LTM method focuses exclusively on endogenously generated behaviour, which is a distinctive feature of system dynamics [47]. The LTM method has a drawback in that model in equilibrium cannot be analysed using the method because, when a model is in equilibrium (a stock's inflow and outflow are equal), all loop scores are defined to be zero. The drawback does not invalidate the LTM method because alternate approaches can address this problem, for example, by offsetting the model state from its equilibrium using a STEP function or some other modelling construct to expose dynamic behaviour [47].

3.2. LTM Method

The LTM method measures loop dominance across the entire model and an important part of this is the link scores and loop scores, which are calculated at each time interval during the model simulation run [47]. While individual loop scores can become quite large, they can be normalised to simplify analysis. This normalised loop score (relative loop score) determines the loop behaviour at a point in time, and the following terms are used:

- The link score is computed for stocks, connectors, and flows. It measures the contribution and polarity of a link between an independent variable and a dependent variable;
- The loop score is computed as a product of link scores. It measures the contribution of a feedback loop to the behaviour of the model and is indicative of the feedback polarity;
- The relative loop score is a normalised loop score measure taking on a value between -1 and 1 . It reports the polarity and fractional contribution of a feedback loop to the change in the value of all stocks at a point in time [47].

The link score is not a general metric that can be used to describe the contribution of any specific link in isolation and must be considered in the context of the loops. The link score can be calculated from stock to flow, flow to a stock, connector to flow, and stock to a connector. Schoenberg et al. [47] presented two methods to calculate the link score: (1) for the links, which do not constitute an integration process, for instance, a link from one auxiliary to another, and (2) for the links from one flow to stock, which is an integration process. Both methods produce a link score, and these link scores are directly comparable and are multiplied together to produce loop scores [47]. In 2021, Schoenberg et al. [48] improved the method to calculate the link score for the links from one flow to stock (with integration). Sensitivity analysis, when combined with LTM, can be used to explore the impact of different parameter values on the model's feedback loops, and this approach is taken in our paper. The LTM method is used to explore the loop dominance behaviour in our model, and a motivating example to illustrate the LTM method and model behaviour analysis is presented in the Supplementary Materials.

3.3. The Misinformation/Disease Model Structure

The misinformation/disease model is based on the well-known SIR structure and is shown in Figure 1, with the misinformation model structure at the top, and the disease model is below. In the disease model, the total population is divided into four stocks or compartments: (i) Susceptible Disease (1) individuals are at risk from the infectious disease; (ii) Infected Disease (2) individuals are infected with the infectious disease and spreading it; (iii) Recovered Disease (3) individuals have recovered and are no longer infectious; and (iv) Total Vaccinated (4) individuals are immune due to vaccination. In the misinformation model, the total population is divided into three stocks or compartments: (i) Susceptible Vaccine Misinformation (15) individuals are at risk of misinformation; (ii) Infected Vaccine Misinformation (16) individuals are infected and spreading misinformation; and (iii) Recovered Vaccine Misinformation (17) individuals no longer spread misinformation.

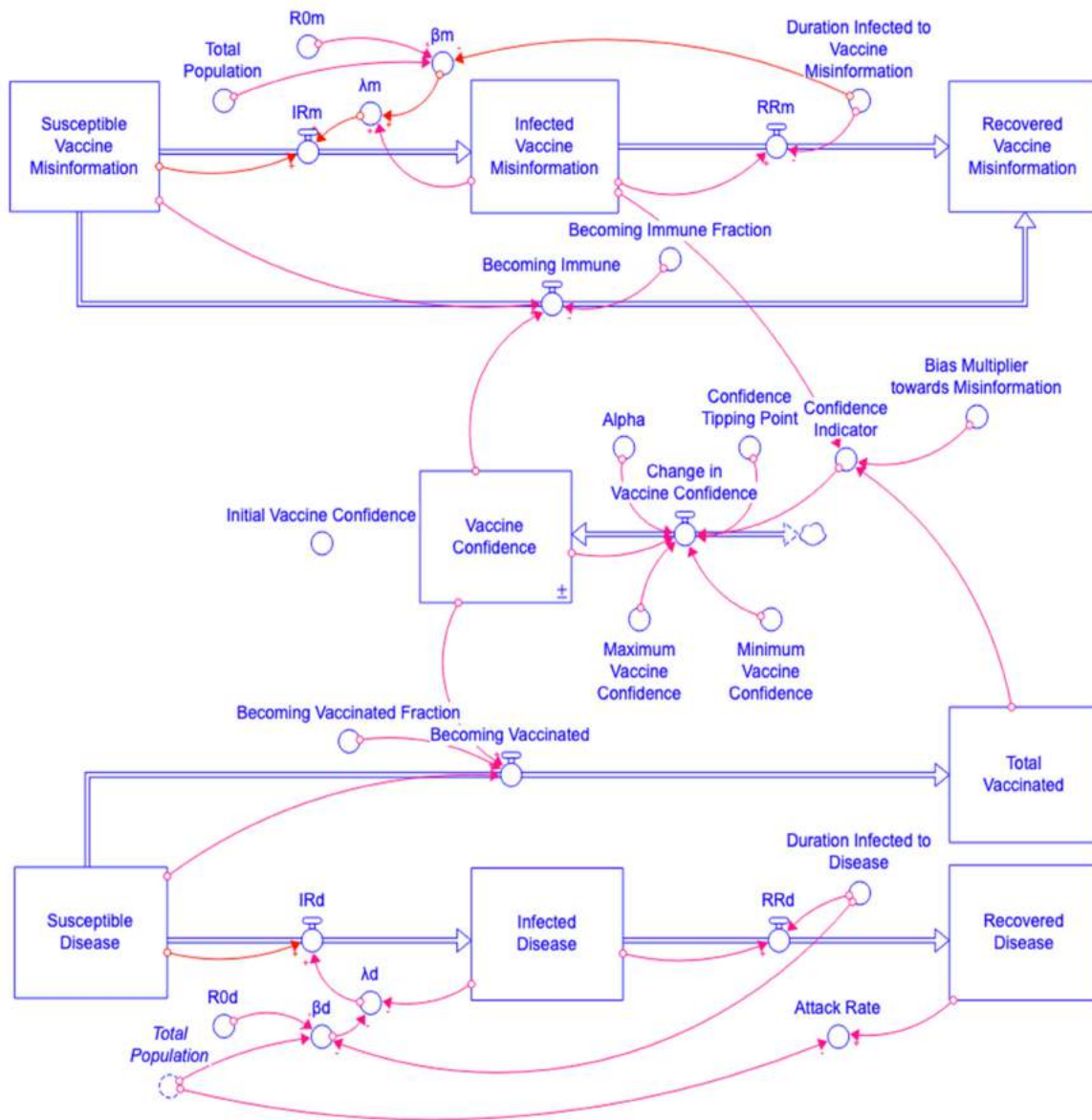


Figure 1. Overview of the misinformation/disease Model.

In the disease model, pathogen spread is caused by social contact. The Total Population (5) size is 10,000 people with 9999 initially placed in the Susceptible Disease stock, 1 in Infected Disease, and 0 initially in Recovered Disease (3) and also in Total Vaccinated (4). The disease model’s differential equations are (1)–(4) and the sum of all four stocks is equal to the Total Population.

$$d(\text{Susceptible Disease}(t))/dt = - \text{Susceptible Disease}(t) \times \lambda_d - \text{Susceptible Disease}(t) \times \text{Becoming Vaccinated Fraction} \times \text{Vaccine Confidence}(t) \tag{1}$$

$$d(\text{Infected Disease}(t))/dt = \text{Susceptible Disease}(t) \times \lambda_d - \text{Infected Disease}(t)/\text{Duration Infected to Disease} \tag{2}$$

$$d(\text{Recovered Disease}(t))/dt = \text{Infected Disease}(t)/\text{Duration Infected to Disease} \tag{3}$$

$$d(\text{Total Vaccinated}(t))/dt = \text{Susceptible Disease}(t) \times \text{Becoming Vaccinated Fraction} \times \text{Vaccine Confidence}(t) \tag{4}$$

$$\text{Total Population} = 10,000 \tag{5}$$

The model’s auxiliaries and flows are shown in Equations (6)–(14). The disease reproduction number R_{0d} (6) is an input to the disease model and is used to determine the per capita contact rate β_d (8). R_{0d} is the average number of secondary disease-infectious

cases that one case generates in a fully susceptible population. In this model, R_{0d} is set to 3 given that the R_0 plausible value for the spread of influenza infectious diseases is between 1.5–4 [49]. The infection rate IR_d (10) of disease is the product of the force of infection λ_d (9) and Susceptible Disease (1). The recovery rate RR_d (11) of disease is a function of Infected Disease (2) and the recovery time Duration Infected to Disease (7). A vaccination policy is included in the model to make individuals immune from infectious diseases. The Becoming Vaccinated flow (13) is defined by Susceptible Disease (1), Becoming Vaccinated Fraction (12), and Vaccine Confidence (34). The disease model's Attack Rate (14) is the proportion of individuals who get infected throughout the full simulation run.

$$R_{0d} = 3 \quad (6)$$

$$\text{Duration Infected to Disease} = 3 \quad (7)$$

$$\beta_d = R_{0d} / (\text{Duration Infected to Disease} \times \text{Total Population}) \quad (8)$$

$$\lambda_d = \beta_d \times \text{Infected Disease}(t) \quad (9)$$

$$IR_d = \lambda_d \times \text{Susceptible Disease}(t) \quad (10)$$

$$RR_d = \text{Infected Disease}(t) / \text{Duration Infected to Disease} \quad (11)$$

$$\text{Becoming Vaccinated Fraction} = 0.05 \quad (12)$$

$$\text{Becoming Vaccinated} = \text{Susceptible Disease}(t) \times \text{Becoming Vaccinated Fraction} \times \text{Vaccine Confidence}(t) \quad (13)$$

$$\text{Attack Rate} = \text{Recovered Disease}(t) / \text{Total Population} \quad (14)$$

The misinformation model is also based on the SIR structure. The spread of misinformation is modelled as a contagious process, which can transmit from infectious misinformation individuals to susceptible misinformation individuals through social contact (which would include contact between people over social media platforms). In the misinformation model, the population size is 10,000 people, with 9999 initially in the stock Susceptible Vaccine Misinformation (15), 1 initially in Infected Vaccine Misinformation (16), and 0 initially Recovered Vaccine Misinformation (17).

$$d(\text{Susceptible Vaccine Misinformation}(t)) / dt = -\text{Susceptible Vaccine Misinformation}(t) \times \lambda_m - \text{Susceptible Vaccine Misinformation}(t) \times \text{Becoming Immune Fraction} \times \text{Vaccine Confidence}(t) \quad (15)$$

$$d(\text{Infected Vaccine Misinformation}(t)) / dt = \text{Susceptible Vaccine Misinformation}(t) \times \lambda_m - \text{Infected Vaccine Misinformation}(t) / \text{Duration Infected to Vaccine Misinformation} \quad (16)$$

$$d(\text{Recovered Vaccine Misinformation}(t)) / dt = \text{Infected Vaccine Misinformation}(t) / \text{Duration Infected to Vaccine Misinformation} + \text{Susceptible Vaccine Misinformation}(t) \times \text{Becoming Immune Fraction} \times \text{Vaccine Confidence}(t) \quad (17)$$

The rumour reproduction number R_{0m} (18) is an input to the model and drives the per capita contact value β_m (20). R_{0m} is an average number of secondary misinformation infectious cases that one misinformation infected case would generate in the total misinformation susceptible population. In this research, the R_{0m} is initially set to 12, which is based on indicative values from rumour models [25,26,28]. The infection rate IR_m (22) for misinformation is the product of the force of infection λ_m (21) and Susceptible Vaccine Misinformation (15). The recovery rate RR_m (23) of misinformation is a function of Infected Vaccine Misinformation (16) and Duration Infected to Vaccine Misinformation (19). Normally, when people have high vaccine confidence then there is a beneficial side effect, which improves an individual's immunity from misinformation. Therefore, the Susceptible Vaccine Misinformation individuals move into the Recovered Vaccine Misinformation via Becoming Immune flow (25). Hence, the Becoming Immune flow is defined by Susceptible Vaccine Misinformation (15), Becoming Immune Fraction (24) and Vaccine Confidence (34).

$$R_{0m} = 12 \quad (18)$$

$$\text{Duration Infected to Vaccine Misinformation} = 60 \quad (19)$$

$$\beta_m = R_{0m} / (\text{Duration Infected to Vaccine Misinformation} \times \text{Total Population}) \quad (20)$$

$$\lambda_m = \beta_m \times \text{Infected Vaccine Misinformation}(t) \quad (21)$$

$$IR_m = \lambda_m \times \text{Susceptible Vaccine Misinformation}(t) \quad (22)$$

$$RR_m = \text{Infected Vaccine Misinformation}(t) / \text{Duration Infected to Vaccine Misinformation} \quad (23)$$

$$\text{Becoming Immune Fraction} = 0.05 \quad (24)$$

$$\text{Becoming Immune} = \text{Susceptible Vaccine Misinformation}(t) \times \text{Becoming Immune Fraction} \times \text{Vaccine Confidence}(t) \quad (25)$$

3.4. The Misinformation/Disease Model Interaction

The success of a vaccination program depends on population vaccine confidence [11], which is influenced by individuals and their environment [29], and also fluctuates due to vaccine-related misinformation [12]. This causal structure is captured in the model, as the misinformation and disease models are connected through the Vaccine Confidence (34) stock, which is a goal seeking structure that has two possible end points: a minimum value and maximum value. The Minimum Vaccine Confidence (31) represents the lowest vaccine confidence level, while the Maximum Vaccine Confidence (32) represents the highest level. The Confidence Indicator (28) is defined by the Total Vaccinated (4) stock, Infected Vaccine Misinformation (16) stock, and a Bias Multiplier towards Misinformation (27). In the model, the Change in Vaccine Confidence (33) is a goal seeking flow defined by the Confidence Indicator (28), Confidence Tipping Point (30), Minimum Vaccine Confidence (31), Maximum Vaccine Confidence (32), Alpha (29), and Vaccine Confidence (34).

$$\text{Initial Vaccine Confidence} = 0.8 \quad (26)$$

$$\text{Bias Multiplier towards Misinformation} = 100 \quad (27)$$

$$\text{Confidence Indicator} = \text{Total Vaccinated}(t) / (\text{Total Vaccinated}(t) + \text{Infected Vaccine Misinformation}(t) \times \text{Bias Multiplier towards Misinformation}) \quad (28)$$

$$\text{Alpha} = 1 \quad (29)$$

$$\text{Confidence Tipping Point} = 0.7 \quad (30)$$

$$\text{Minimum Vaccine Confidence} = 0.1 \quad (31)$$

$$\text{Maximum Vaccine Confidence} = 0.9 \quad (32)$$

$$\text{Change in Vaccine Confidence} = \text{IF Confidence Indicator} \geq \text{Confidence Tipping Point THEN Alpha} \times (\text{Maximum Vaccine Confidence} - \text{Vaccine Confidence}(t)) \text{ ELSE Alpha} \times (\text{Minimum Vaccine Confidence} - \text{Vaccine Confidence}(t)) \quad (33)$$

$$d(\text{Vaccine Confidence}(t))/dt = \text{IF Confidence Indicator} \geq \text{Confidence Tipping Point THEN Alpha} \times (\text{Maximum Vaccine Confidence} - \text{Vaccine Confidence}(t)) \text{ ELSE Alpha} \times (\text{Minimum Vaccine Confidence} - \text{Vaccine Confidence}(t)) \quad (34)$$

3.5. The Misinformation/Disease Model Feedback Loops

The model has a total of 11 feedback loops, which contribute to the model behaviour. The reinforcing and balancing loops are divided into two categories based on contagion processes and depletion processes. The contagion process involves the spreading of an infectious disease or misinformation in a group of people. The depletion process suppresses an infectious disease or misinformation in a group of people. Figure 2 shows an overview of the model's feedback loops, based on a causal loop diagram, which is useful for showing the feedback structures.

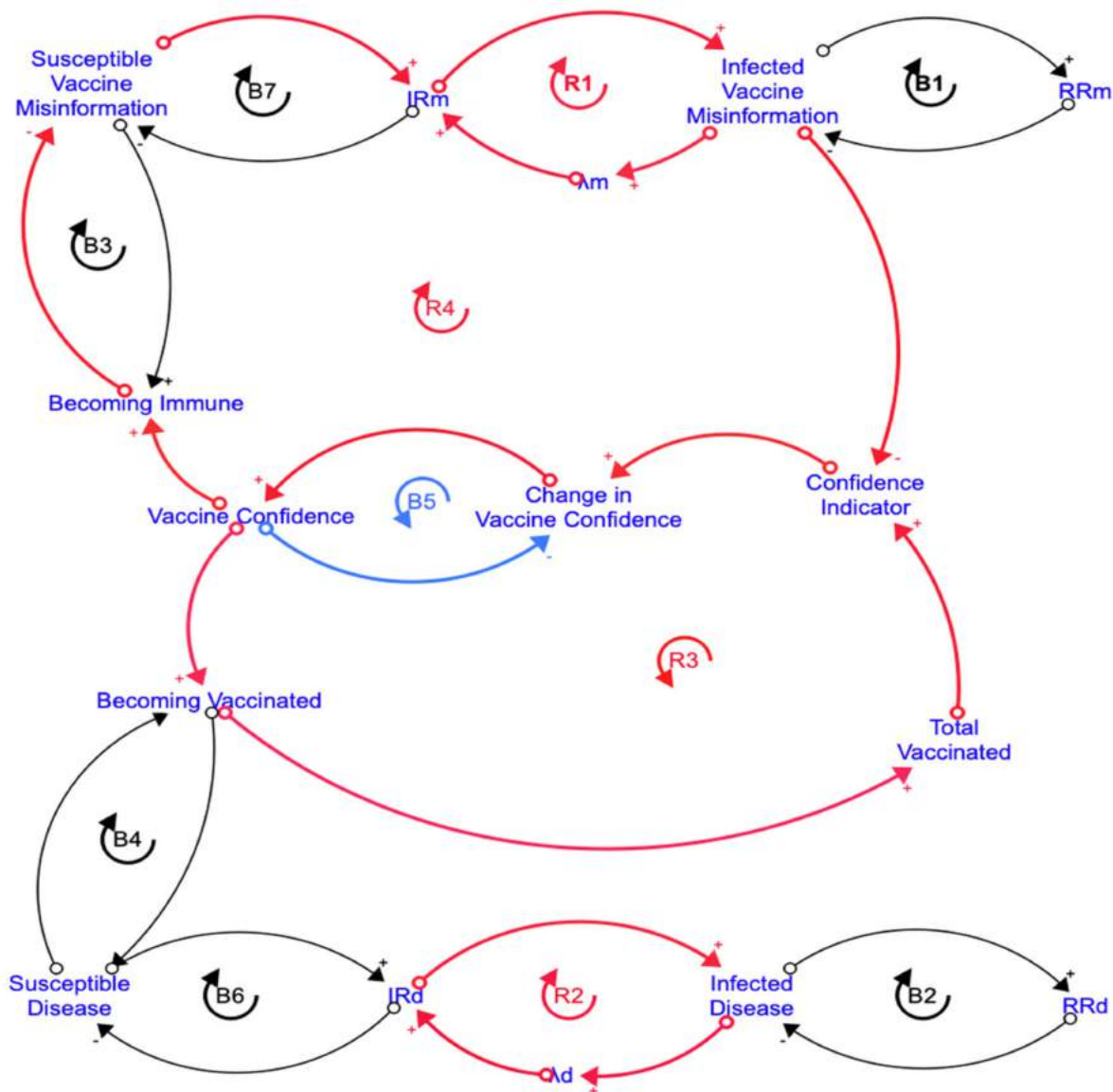


Figure 2. The misinformation/disease model’s feedback loops.

The model behaviour is generated by the misinformation model’s 4 feedback loops and the disease model’s 4 feedback loops. The remaining 3 feedback loops are interactions between both elements through the Vaccine Confidence stock. The above Figure 2 shows that loop R₃ loop consists of 2 stocks and 5 variables. It is a reinforcing loop between the two stocks: Vaccine Confidence and Total Vaccinated. It shows that vaccinated individuals strengthen vaccine confidence and higher vaccine confidence supports the vaccination process. Loop R₄ consists of 3 stocks and 7 variables. It is a reinforcing loop between the three stocks: Vaccine Confidence, Susceptible Vaccine Misinformation, and Infected Vaccine Misinformation. It indicates that an increase in vaccine confidence decreases the spread of vaccine misinformation, which in turn, boosts vaccine confidence. The B₅ loop consists of 1 stock and 2 variables. It is a balancing loop between Vaccine Confidence and Change in Vaccine Confidence. It shows that a change in vaccine confidence flow adjusts the vaccine confidence level and balances system behaviour. Table 1 lists all the reinforcing and balancing feedback loop numbers, the process description, the loop’s stocks, and the variables’ details.

Table 1. The misinformation/disease model’s 11 feedback loops. Positive links are shown in red and negative links are shown in blue.

Loop ID	Loop Description	Loop Variables
R ₁	Misinformation contagion process	Infected Vaccine Misinformation → λ _m → IR _m → Infected Vaccine Misinformation
R ₂	Disease contagion process	Infected Disease → λ _d → IR _d → Infected Disease
R ₃	Vaccine Confidence leads to more vaccinations, which in turn increase Vaccine Confidence	Vaccine Confidence → Becoming Vaccinated → Total Vaccinated → Confidence Indicator → Change in Vaccine Confidence → Vaccine Confidence
R ₄	Vaccine Confidence reduces the spread of misinformation, which increases Vaccine Confidence	Vaccine Confidence → Becoming Immune → Susceptible Vaccine Misinformation → IR _m → Infected Vaccine Misinformation → Confidence Indicator → Change in Vaccine Confidence → Vaccine Confidence
B ₁	Misinformation recovery	Infected Vaccine Misinformation → RR _m → Infected Vaccine Misinformation
B ₂	Disease recovery	Infected Disease → RR _d → Infected Disease
B ₃	Immune to misinformation reduces misinformation vulnerability	Susceptible Vaccine Misinformation → Becoming Immune → Susceptible Vaccine Misinformation
B ₄	Vaccination reduces disease vulnerability	Susceptible Disease → Becoming Vaccinated → Susceptible Disease
B ₅	Vaccine confidence adjustment	Vaccine Confidence → Change in Vaccine Confidence → Vaccine Confidence
B ₆	Depletion disease	Susceptible Disease → IR _d → Susceptible Disease
B ₇	Depletion misinformation	Susceptible Vaccine Misinformation → IR _m → Susceptible Vaccine Misinformation

4. Experimental Results

In this section, we present the model results with (1) nine scenarios (S1 to S9) and (2) sensitivity analysis scenarios (SA1 to SA6). Tables 2 and 3 list the variables; R_{0d}, R_{0m}, and the remaining variables have fixed values. R_{0m} and R_{0d} can vary, and plausible ranges are selected [28,49].

Table 2. Scenarios (S1–S9).

R _{0d} \ R _{0m}	Low Value (L) = 6	Medium Value (M) = 12	High Value (H) = 18
Low Value (L) = 2	S1	S2	S3
Medium Value (M) = 3	S4	S5	S6
High Value (H) = 4	S7	S8	S9

Table 3. Sensitivity analysis (SA1–SA6).

No	R_{0m}	R_{0d}
SA1	$R_{0m} = 6$ (Low)	$R_{0d} = \text{Uniform}$ (2,4)
SA2	$R_{0m} = 12$ (Medium)	$R_{0d} = \text{Uniform}$ (2,4)
SA3	$R_{0m} = 18$ (High)	$R_{0d} = \text{Uniform}$ (2,4)
SA4	$R_{0m} = \text{Uniform}$ (6,18)	$R_{0d} = 2$ (Low)
SA5	$R_{0m} = \text{Uniform}$ (6,18)	$R_{0d} = 3$ (Medium)
SA6	$R_{0m} = \text{Uniform}$ (6,18)	$R_{0d} = 4$ (High)

4.1. Exploring a Range of R_0 Values

The disease attack rate is the proportion of people who are infected with a disease in a population, and this is an output measure from the model. The first set of experiments is based on scenarios S1 to S9, and the attack rate results are shown in Figure 3. It highlights the range of results from the lowest impact on the population ($R_{0m} = 6, R_{0d} = 2$) to the highest ($R_{0m} = 18, R_{0d} = 4$). The results show the significant impact of increased misinformation contagion on the disease attack rate. For example, consider the results shown in Table 4 taking one row at a time. They show that by keeping the R_{0d} constant, there is a corresponding increase in the attack rate due to the extra contagion effect from misinformation. For example, for an $R_{0d} = 3$ in S4, the attack rate increases by 75.6% in S6 (from 0.23 to 0.404), thereby showing the sensitivity of the attack rate to increases in R_{0m} . Scenario S9 shows the highest disease Attack Rate, where both R_{0d} and R_{0m} values are at their highest.

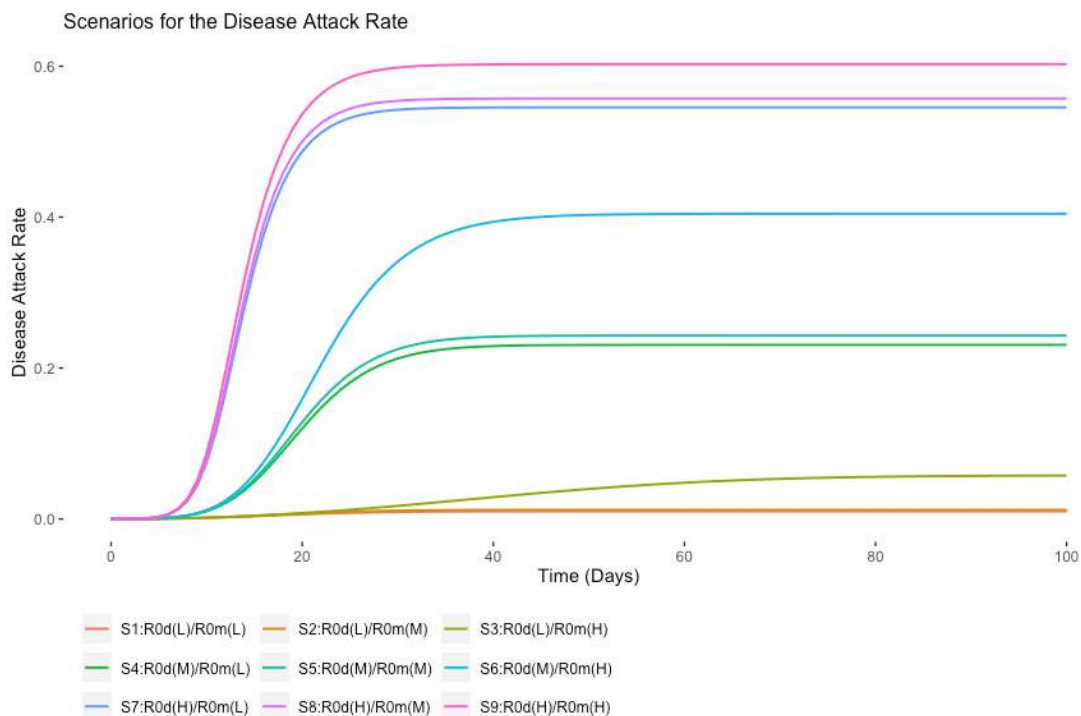


Figure 3. Scenarios (S1–S9) for the disease attack rate.

Table 4. Scenario (S1–S9) results.

R_{0m}	R_{0m}	Low Value (L) = 6	Disease Attack Rate	Medium Value (M) = 12	Disease Attack Rate	High Value (H) = 18	Disease Attack Rate
Low Value (L) = 2		S1	0.01	S2	0.012	S3	0.057
Medium Value (M) = 3		S4	0.23	S5	0.243	S6	0.404
High Value (H) = 4		S7	0.545	S8	0.557	S9	0.602

4.2. Sensitivity Analysis for Scenarios SA1 to SA6

In this section, the second set of experiments is based on sensitivity analysis for scenarios SA1 to SA6. Figure 4 shows box plots for the disease Attack Rate. The main points of interest from the sensitivity analysis are:

- The highest median value for the disease attack rate is scenario SA6, where R_{0d} is fixed at four, and R_{0m} varies between six and eighteen. This shows the potential impact that a strong misinformation contagion process has on the outcome;
- Scenario SA1 has the R_{0m} at six, although, even with this low value, the maximum disease attack rate is high at over 40%. This shows reduced vaccine confidence results in lower vaccine uptake;
- Scenario SA3 shows a significant increase in the disease attack rate as compared to SA1 and SA2, where R_{0d} varies between two and four, and R_{0m} is fixed at 18. This shows the impact of high misinformation, which leads to lower vaccine uptake, thereby providing the disease with more opportunities to spread.
- There is an overall pattern whereby varying R_{0m} (SA4, SA5, and SA6) has a higher impact on the disease attack rate than varying R_{0d} (SA1, SA2, and SA3).

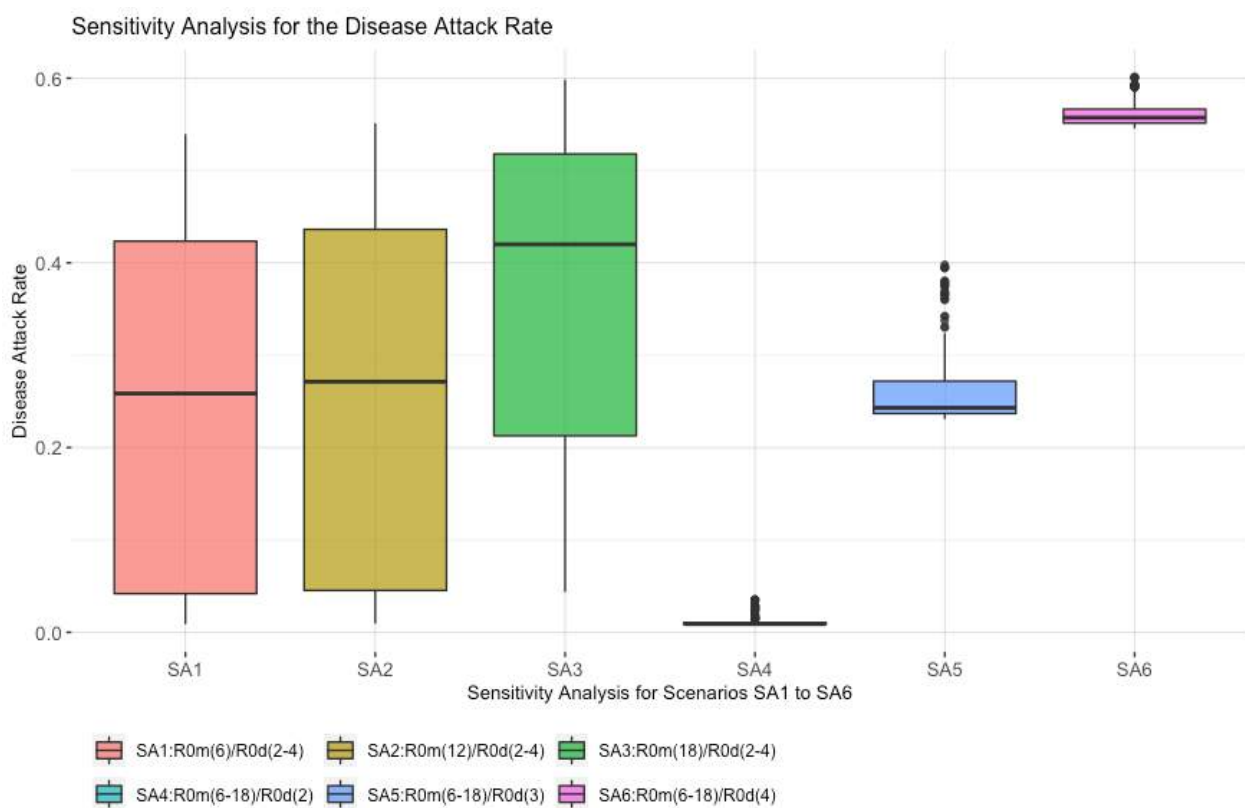


Figure 4. Sensitivity analysis (SA1–SA6) for the disease attack rate.

4.3. The Scenarios S1 to S9 with LTM Analysis

Here, we explore the effect of R_{0m} and R_{0d} on the model’s feedback loops. Figure 5 presents a visual comparison between model runs from two of the scenarios, S2 ($R_{0d} = 2$, $R_{0m} = 12$) and S5 ($R_{0d} = 3$, $R_{0m} = 12$). The area plot displays the contribution of each loop to model behaviour over time, where the total across all loops will add up to 100%. The plots show the feedback loops’ behaviours on the y-axis from 0% to 100% (where 50% is the point where the loop score becomes dominant), and the model run time on the x-axis. The four reinforcing loops (red colour) and seven balancing loops (blue colour) are shown over the entire period of the model’s simulation, T_0 to T_{100} . In both scenarios, S2 and S5, the initial run time from T_0 to T_{30} shows that reinforcing feedback loops cover almost 55% of the area and there are a few points of inflection (POI). In both scenarios, S2 ($R_{0d} = 2$,

$R_{0m} = 12$) and S5 ($R_{0d} = 3, R_{0m} = 12$), the final run time, T_{30} to T_{100} , shows a prominent increase in the balancing feedback loop's coverage. The scenario S2 ($R_{0d} = 2, R_{0m} = 12$) and S5 ($R_{0d} = 3, R_{0m} = 12$) comparisons show minor changes in the reinforcing and balancing feedback loops' behaviours.

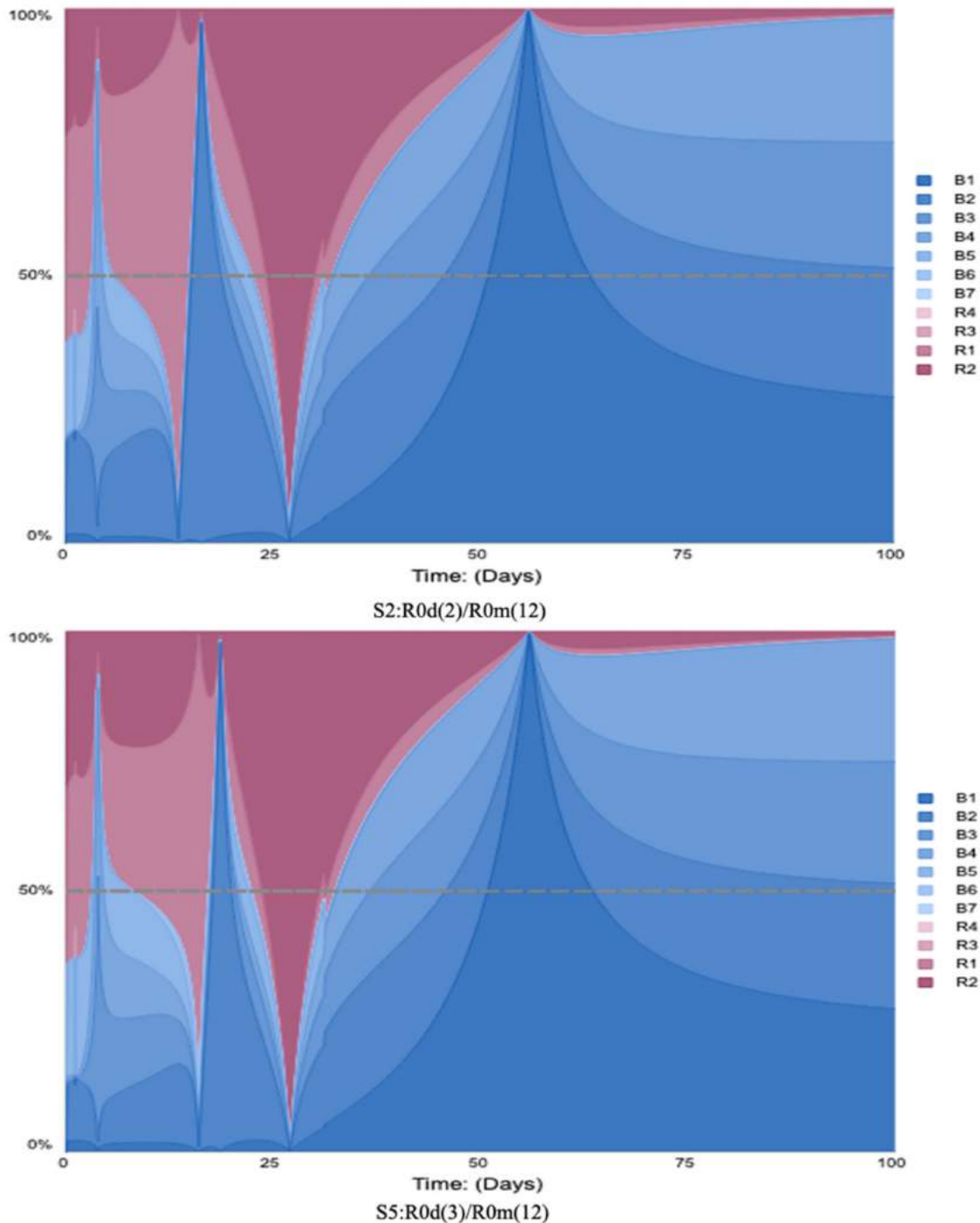


Figure 5. A Comparison between S2 and S5 feedback loop behaviours until T_{100} .

Figure 6 presents another comparison based on scenarios S2 and S3, where R_{0m} varies between 12 and 18, and R_{0d} is fixed at two. The scenarios show a prominent change in the feedback loops' behaviours. In both scenarios, S2 ($R_{0d} = 2, R_{0m} = 12$) and S3 ($R_{0d} = 2, R_{0m} = 18$), the initial run time from T_0 to T_{30} shows that reinforcing feedback loops cover almost 55% of the area. In scenario S3 ($R_{0d} = 2, R_{0m} = 18$), the final run time from T_{30}

to T_{100} shows multiple points of inflection (POI), where the balancing feedback loop area increases but the reinforcing behaviour is continues to have an influence, as they still cover almost 40% of the area (e.g., loop R_1), which is due to the impact of high misinformation. Therefore, a higher misinformation scenario can be seen to increase reinforcing behaviour and decrease balancing behaviour.

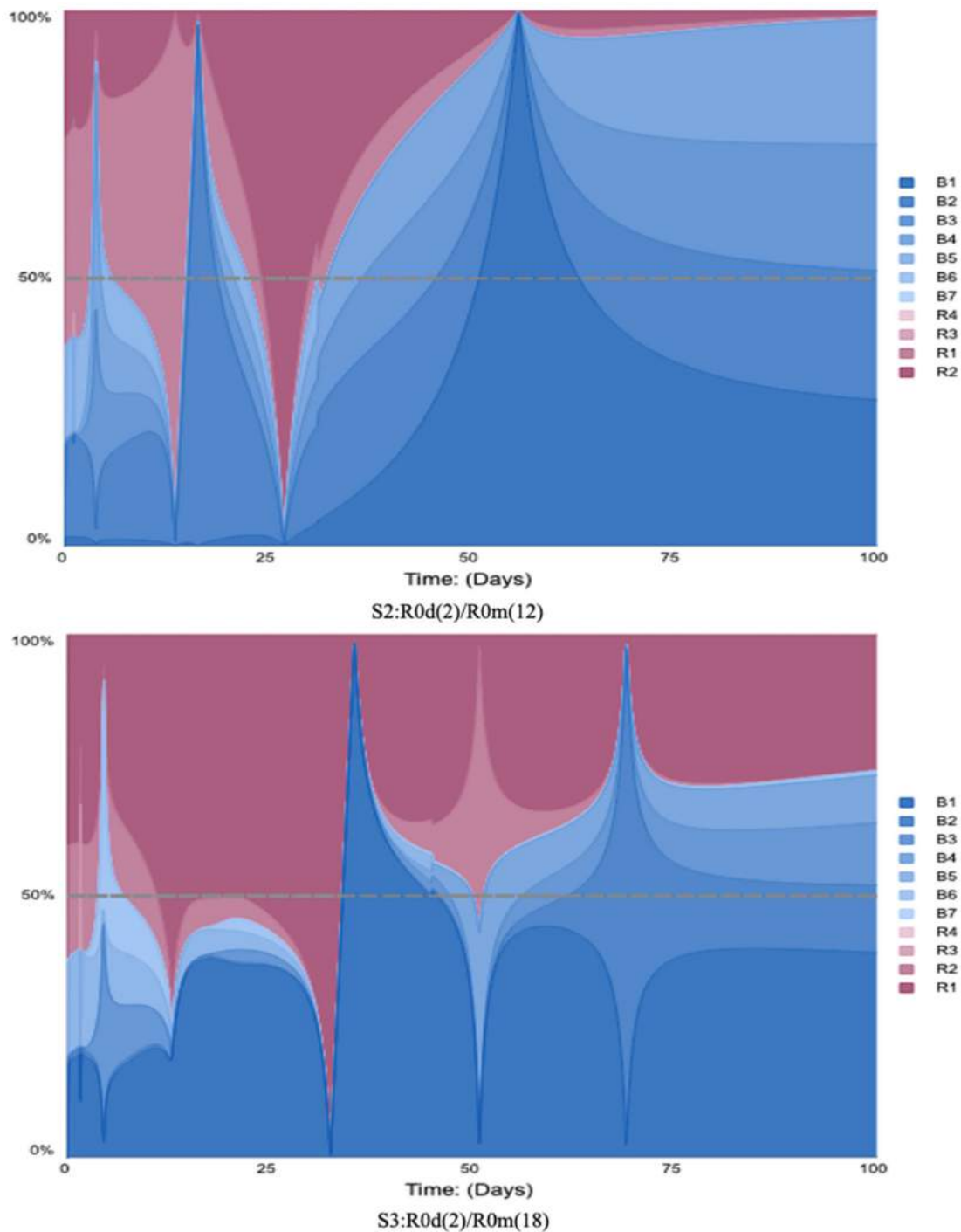


Figure 6. A comparison between S2 and S3 feedback loop behaviours until T_{100} .

Table 5 summarises the total of all the reinforcing and balancing feedback loops’ average relative scores. Figure 7 presents all the scenarios (S1 to S9) to show the effect of R_{0m} and R_{0d} on the model’s reinforcing and balancing feedback loops’ behaviours and the following results are of interest:

- When R_{0d} is fixed at two, and R_{0m} varies between 12 and 18, scenarios S1, S2, and S3 show a notable change in the reinforcing loops' average relative scores, from 17% to 41%. However, with R_{0m} fixed at six, when R_{0d} varies, (S1, S4, and S7) the reinforcing loops' average relative scores do not increase. This suggests that the variation in R_{0m} has a bigger impact on the reinforcing loops' dominance;
- When R_{0d} equals three and R_{0m} varies between six and eighteen (S4, S5, and S6), the reinforcing loops' average relative scores change from 18% to 29%. With R_{0m} fixed at 12 (S2, S5, and S8), the reinforcing contribution increases from 24% to 42%;
- When R_{0d} equals four, and R_{0m} varies between 12 and 18 (S7, S8, and S9), the reinforcing loops' average relative scores change from 16% to 23%. With R_{0m} fixed at 18 (S3, S6, and S9), the reinforcing contribution decreases from 41% to 23%. The decline in the reinforcing contribution is caused by vaccine confidence stock, which is a goal-seeking structure. The result shows that high disease and misinformation impact model feedback loops scores and the vaccine confidence stock's goal-seeking structure adjust the vaccine confidence level.

Overall, the results show that increases in R_{0m} and R_{0d} impact the dominant share of the reinforcing and balancing feedback loops.

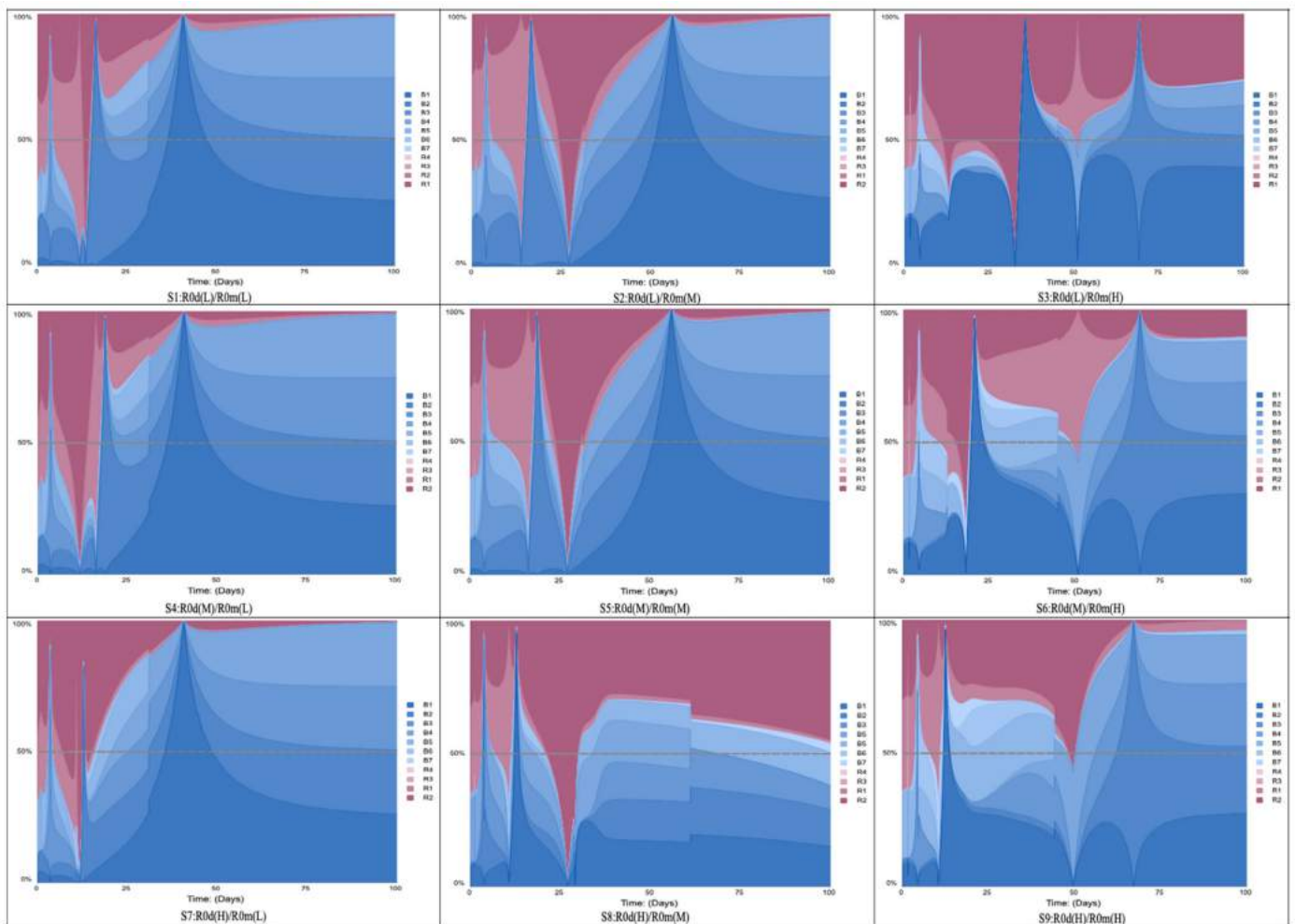


Figure 7. A comparison between feedback loops behaviour from S1 to S9.

Table 5. Scenario (S1–S9) results.

R_{0d}	R_{0m}	Low Value (L) = 6	Feedback Loop's Score	Medium Value (M) = 12	Feedback Loop's Score	High Value (H) = 18	Feedback Loop's Score
Low Value (L) = 2		S1	R = 17.69% B = 82.31%	S2	R = 24.19% B = 75.81%	S3	R = 41.21% B = 58.79%
Medium Value (M) = 3		S4	R = 18.1% B = 81.9%	S5	R = 24.06% B = 75.94%	S6	R = 29.57% B = 70.43%
High Value (H) = 4		S7	R = 16.26% B = 83.74%	S8	R = 42.03% B = 57.97%	S9	R = 23.16% B = 76.84%

4.4. Sensitivity Analysis SA1 to SA6 Combined with LTM

In this section, we explore the R_{0m} and R_{0d} on the model's feedback loops' behaviours using sensitivity analysis combined with LTM. The analysis is based on the sensitivity analysis for scenarios SA1 through to SA6. The experiment varies R_{0m} and R_{0d} to explore the impact on the negative feedback loop B_5 (vaccine confidence adjustment). Figure 8 presents the scenarios (SA1 to SA6) to show impact on the negative feedback loop B_5 (vaccine confidence adjustment).

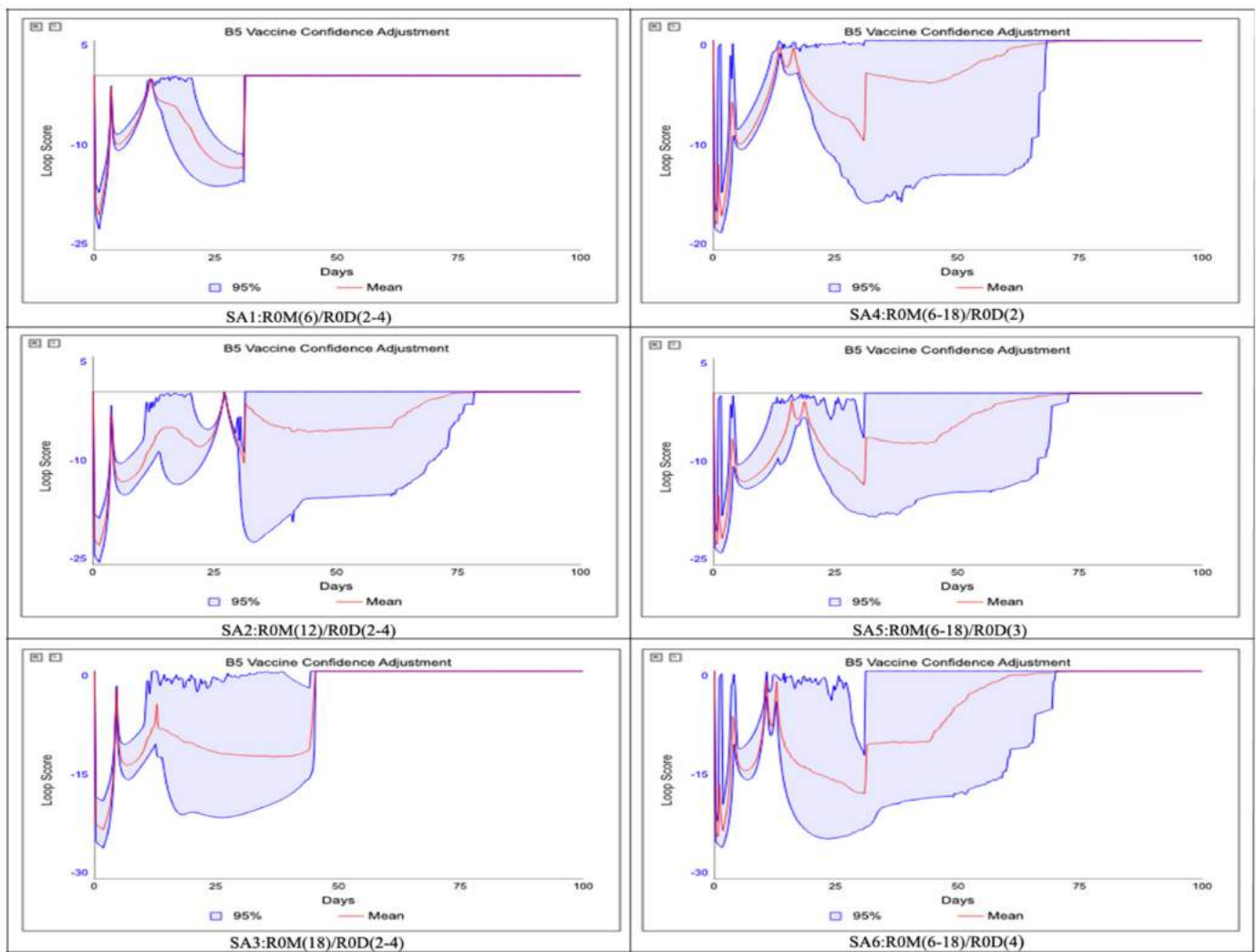


Figure 8. Sensitivity analysis (SA1–SA6) combined with LTM.

This loop is selected as it plays an important role in the model behaviour. It consists of Vaccine Confidence stock and Change in Vaccine Confidence flow, and the misinformation and disease parts of the model are connected through the Vaccine Confidence stock. The main points of interest from the sensitivity analysis combined with LTM are:

- Scenario SA6 shows the highest impact for the B_5 (vaccine confidence adjustment) feedback loop, where R_{0d} is fixed at four, and R_{0m} varies between six and eighteen. The B_5 (vaccine confidence adjustment) feedback loop's relative score increases by more than -25% . This shows the potential impact of the misinformation contagion process;
- Scenario SA1 shows the least impact for the B_5 (vaccine confidence adjustment) feedback loop, where R_{0m} is fixed at six, and R_{0d} varies between two and four, although even with this low value, the B_5 (vaccine confidence adjustment) feedback loop's relative score increases by almost -22% . This shows the impact of reduced vaccine confidence, leading to a change in the vaccine confidence rate;
- Scenario SA3 also shows an impact on the B_5 (vaccine confidence adjustment) feedback loop, where R_{0d} varies between two and four, and R_{0m} is fixed at 18. The B_5 (vaccine confidence adjustment) feedback loop's relative score is almost -25% . This shows the effect of high misinformation, leading to lower vaccine uptake;
- Scenario SA4 shows an increase for the B_5 (vaccine confidence adjustment) feedback loop score, where R_{0d} is fixed at two, and R_{0m} varies between six and eighteen, although, even with this low value of R_{0d} , the B_5 (vaccine confidence adjustment) feedback loop's relative score increases by almost -19% . This shows the impact of R_{0m} and R_{0d} , leading to change in the vaccine confidence and disease attack rate;
- The analysis shows a pattern whereby varying R_{0m} (SA4, SA5, and SA6) has a higher impact on the loop score for B_5 (vaccine confidence adjustment) and disease attack rate, as well than varying R_{0d} (SA1, SA2, and SA3).

5. Conclusions

In the past, epidemiological models failed to account for the important aspect of behavioural responses to diseases in human populations [21]. Our research focuses on this gap by combining into a model two diffusion dynamics, the spread of misinformation and the spread of disease, each of which has different reproduction numbers. We have seen from our literature review that the spread of misinformation can affect and decrease vaccine intention [50], that lower levels of vaccine confidence is a threat to global health, and that "online social media can act as an "echo chamber" where personal opinions that affect individual medical decisions are predominately reaffirmed by others" [51].

This paper's experiments applied sensitivity and loop impact analysis to explore the model's behaviour and identify the driving forces or variables behind the model's behaviour. Our results showed that even low R_{0m} escalated the disease Attack Rate, whereas higher R_{0m} more significantly increased the disease Attack Rate. The model feedback loops analysis also indicated that R_{0m} affected the reinforcing and balancing feedback loops' relative scores and increased the disease Attack Rate. Sensitivity analysis combined with LTM establishes confidence in the usefulness of this model, as it shows how misinformation can significantly impact the disease attack rate.

From a policy perspective, the model highlights the importance of understanding the inter-relationships between the contagion dynamics of misinformation and the spread of diseases. In the context of a fast-moving pathogen, the model's results indicate the importance of the speed of response and building population confidence in vaccines, a message that is consistent with recently published modelling work that highlights the urgent need for effective interventions to increase trust and inform the public [21]. There may also be opportunities for enhancing education opportunities for schools, for example, by introducing simple SIR models as part of the mathematics curriculum, and also by using these models to demonstrate the positive impact that human behaviour (mask wearing, vaccination uptake, and resilience to misinformation) can have on overall public health.

While the research results are informative and provide valuable insights to highlight the impact of misinformation on disease transmission, there is scope for future work with the model. This would focus on three areas: (1) applying the model to a country-specific case study, involving measuring and assessing key parameters, such as R_0 and the results of vaccine confidence surveys; (2) extending the model to different age cohorts to explore heterogeneities between a range of groups in terms of vaccine confidence and disease spread; and (3) extending the loop dominance analysis to include techniques such as the eigenvalue elasticity analysis, (EEA) and the partway participation method (PPM).

Supplementary Materials: The following supporting information can be downloaded at: <https://www.mdpi.com/article/10.3390/systems10020050/s1>, Figure S1. SI Model Structure. Figure S2. R_1 and B_1 Loops' Relative Scores in Line Plot. Figure S3. R_1 and B_1 Loops' Relative Scores in Stacked Area Plot. Figure S4. The R_1 and B_1 Relative Loops' Scores against S and I Stocks. Table S1. The R_1 and B_1 Loops' Details. Table S2. Demonstration Link Scores for $S \rightarrow IR$, $\lambda \rightarrow IR$ and $I \rightarrow \lambda$ by using Equation (S1). Calculations are based on the equations: $IR = S * \lambda$ and $\lambda = I * \beta$. Table S3. Demonstration Link Scores for $IR \rightarrow S$ and $IR \rightarrow I$ by using Equation (S2). Table S4. Demonstration Loop Scores and Relative Loop Scores for the B_1 and R_1 .

Author Contributions: Research conceptualisation, methodology, investigation, visualisation, conclusion, formal analysis and writing original draft, N.M.; formal analysis and paper editing, C.G.; research supervision, formal analysis, and paper editing, J.D. All authors have read and agreed to the published version of the manuscript.

Funding: College of Science and Engineering Postgraduate Research Scholarship. The project has also received funding from the European Union's Horizon 2020 Research and Innovation programme under the Grant Agreement No. 883285. The material presented and views expressed here are the responsibility of the author(s) only. The EU Commission takes no responsibility for any use made of the information set out.

Conflicts of Interest: The authors declare no conflict of interest.

References

1. Bloom, B.R.; Marcuse, E.; Mnookin, S. Addressing Vaccine Hesitancy. *Science* **2014**, *344*, 339. [CrossRef] [PubMed]
2. Morens, D.M.; Fauci, A.S. Emerging Infectious Diseases: Threats to Human Health and Global Stability. *PLoS Pathog.* **2013**, *9*, e1003467. [CrossRef] [PubMed]
3. CDC. List of Vaccines Used in United States. Available online: <https://www.cdc.gov/vaccines/vpd/vaccines-list.html> (accessed on 6 April 2022).
4. Wolfe, R.; Sharp, L. Anti-vaccinationists Past and Present. *BMJ* **2002**, *325*, 430–432. [CrossRef] [PubMed]
5. Rosselli, R.; Martini, M.; Bragazzi, N.L. The old and the new: Vaccine hesitancy in the era of the Web 2.0. Challenges and opportunities. *J. Prev. Med. Hyg.* **2016**, *57*, E47–E50.
6. MacDonald, N.E.; Eskola, J.; Liang, X.; Chaudhuri, M.; Dube, E.; Gellin, B.; Goldstein, S.; Larson, H.; Manzo, M.L.; Reingold, A.; et al. Vaccine Hesitancy: Definition, Scope and Determinants. *Vaccine* **2015**, *33*, 4161–4164. [CrossRef]
7. Lorini, C.; Santomauro, F.; Donzellini, M.; Capecci, L.; Bechini, A.; Boccalini, S.; Bonanni, P.; Bonaccorsi, G. Health literacy and vaccination: A systematic review. *Hum. Vaccines Immunother.* **2018**, *14*, 478–488. [CrossRef]
8. Larson, H. Prof Heidi Larson (LSHTM) on Her Book Stuck: How Vaccine Rumors Start—And Why They Don't Go Away. Online Interview. 2020. Available online: <https://www.youtube.com/watch?v=MM-JiQhYDbw> (accessed on 15 October 2020).
9. Larson, H.J.; Jarrett, C.; Eckersberger, E.; Smith, D.M.D.; Paterson, P. Understanding Vaccine Hesitancy around Vaccines and Vaccination from a Global Perspective: A Systematic Review of Published Literature, 2007–2012. *Vaccine* **2014**, *32*, 2150–2159. [CrossRef]
10. Who.Int. Addressing Vaccine Hesitancy. Available online: https://www.who.int/immunization/sage/meetings/2014/october/3_SAGE_WG_Strategies_addressing_vaccine_hesitancy_2014.pdf (accessed on 15 February 2020).
11. Karafillakis, E.; Larson, H.J. The benefit of the doubt or doubts over benefits? A systematic literature review of perceived risks of vaccines in European populations. *Vaccine* **2017**, *35*, 4840–4850. [CrossRef]
12. Wiyeh, A.B.; Cooper, S.; Nnaji, C.A.; Wiysonge, C.S. Vaccine hesitancy 'outbreaks': Using epidemiological modeling of the spread of ideas to understand the effects of vaccine related events on vaccine hesitancy. *Expert Rev. Vaccines* **2018**, *17*, 1063–1070. [CrossRef]
13. Tafuri, S.; Gallone, M.S.; Cappelli, M.G.; Martinelli, D.; Prato, R.; Germinario, C. Addressing the anti-vaccination movement and the role of HCWs. *Vaccine* **2014**, *32*, 4860–4865. [CrossRef]
14. Davies, P.; Chapman, S.; Leask, J. Antivaccination Activists on the World Wide Web. *Arch. Dis. Child.* **2002**, *87*, 22–25. [CrossRef]

15. Celentano, D.D.; Thomas, W.V. Social Networks and Health: Models, Methods, and Applications. *Am. J. Epidemiol.* **2010**, *172*, 488. [CrossRef]
16. Larson, H.J.; De Figueiredo, A.; Xiaohong, Z.; Schulz, W.S.; Verger, P.; Johnston, I.G.; Cook, A.R.; Jones, N.S. The State of Vaccine Confidence 2016: Global Insights Through a 67-Country Survey. *eBioMedicine* **2016**, *12*, 295–301. [CrossRef]
17. Lahouati, M.; De Coucy, A.; Sarlangue, J.; Cazanave, C. Spread of vaccine hesitancy in France: What about YouTube™? *Vaccine* **2020**, *38*, 5779–5782. [CrossRef]
18. The Guardian. I'm Not an Anti-Vaxxer, but US Health Workers' Vaccine Hesitancy Raises Alarm. Available online: <https://www.theguardian.com/world/2021/jan/10/coronavirus-covid-19-vaccine-hesitancy-us-health-workers> (accessed on 10 January 2021).
19. Thaker, J.; Subramanian, A. Exposure to COVID-19 Vaccine Hesitancy Is as Impactful as Vaccine Misinformation in Inducing a Decline in Vaccination Intentions in New Zealand: Results from Pre-Post Between-Groups Randomized Block Experiment. *Front. Commun.* **2021**, *6*, 159. [CrossRef]
20. Law, T. Israel's COVID-19 Vaccination Rollout Is Slowing at a Critical Moment. That's a Warning for the Rest of Us. Time. Available online: <https://time.com/5947967/israel-covid-vaccine-rollout/> (accessed on 8 June 2021).
21. Sontag, A.; Rogers, T.; Yates, C.A. Misinformation can prevent the suppression of epidemics. *J. R. Soc. Interface* **2022**, *19*, 20210668. [CrossRef]
22. Gabriel, C.; Carter, T. Information Transmission Through Human Informants: Simulation. *CASOS* **1996**.
23. Kermack, W.O.; McKendrick, A.G. A contribution to the mathematical theory of epidemics. *Proc. R. Soc. Lond. Ser. A Math. Phys. Sci.* **1927**, *115*, 700–721. [CrossRef]
24. Zhao, X.; Wang, J. Dynamical Model about Rumor Spreading with Medium. *Discret. Dyn. Nat. Soc.* **2013**, *2013*, 586867. [CrossRef]
25. Bettencourt, L.M.; Cintrón-Arias, A.; Kaiser, D.; Castillo-Chavez, C. The power of a good idea: Quantitative modeling of the spread of ideas from epidemiological models. *Phys. A Stat. Mech. Its Appl.* **2006**, *364*, 513–536. [CrossRef]
26. Epstein, J.M.; Parker, J.; Cummings, D.; Hammond, R.A. Coupled Contagion Dynamics of Fear and Disease: Mathematical and Computational Explorations. *PLoS ONE* **2008**, *3*, e3955. [CrossRef]
27. Li, C. A study on time-delay rumor propagation model with saturated control function. *Adv. Differ. Equ.* **2017**, *2017*, 255. [CrossRef]
28. Liu, X.; Li, T.; Tian, M. Rumor spreading of a SEIR model in complex social networks with hesitating mechanism. *Adv. Differ. Equ.* **2018**, *2018*, 391. [CrossRef]
29. Larson, H. *Stuck: Vaccine Rumors Start and Why They Don't Go Away*; Oxford University Press: New York, NY, USA, 2020.
30. Ehrhardt, M.; Gašper, J.; Kilianová, S. SIR-based mathematical modeling of infectious diseases with vaccination and waning immunity. *J. Comput. Sci.* **2019**, *37*, 101027. [CrossRef]
31. Raimundo, S.M.; Yang, H.M.; Engel, A.B. Modelling the effects of temporary immune protection and vaccination against infectious diseases. *Appl. Math. Comput.* **2007**, *189*, 1723–1736. [CrossRef]
32. Hamami, D.; Cameron, R.; Pollock, K.G.; Shankland, C. Waning Immunity Is Associated with Periodic Large Outbreaks of Mumps: A Mathematical Modeling Study of Scottish Data. *Front. Physiol.* **2017**, *8*, 233. [CrossRef]
33. Leung, T.; Campbell, P.; Hughes, B.D.; Frascoli, F.; McCaw, J.M. Infection-acquired versus vaccine-acquired immunity in an SIRWS model. *Infect. Dis. Model.* **2018**, *3*, 118–135. [CrossRef]
34. Nkamba, L.N.; Manga, T.T.; Agouanet, F.; Manyombe, M.L.M. Mathematical model to assess vaccination and effective contact rate impact in the spread of tuberculosis. *J. Biol. Dyn.* **2019**, *13*, 26–42. [CrossRef]
35. Rabiou, M.; Willie, R.; Parumasur, N. Mathematical analysis of a disease-resistant model with imperfect vaccine, quarantine and treatment. *Ric. Mat.* **2020**, *69*, 603–627. [CrossRef]
36. Ghaffarzadegan, N.; Lyneis, J.; Richardson, G.P. How small system dynamics models can help the public policy process. *Syst. Dyn. Rev.* **2010**, *27*, 22–44. [CrossRef]
37. Darabi, N.; Hosseinichimeh, N. System dynamics modeling in health and medicine: A systematic literature review. *Syst. Dyn. Rev.* **2020**, *36*, 29–73. [CrossRef]
38. Serman, J.D. *Business Dynamics: Systems Thinking and Modeling for a Complex World*; McGraw-Hill: New York, NY, USA, 2000.
39. Duggan, J.; Oliva, R. Methods for Identifying Structural Dominance. *Syst. Dyn. Rev.* **2013**, *29*. (Virtual Special Issue). Available online: https://www.researchgate.net/publication/272823783_Methods_of_identifying_structural_dominance (accessed on 9 June 2021).
40. Ford, D. A behavioral approach to feedback loop dominance analysis. *Syst. Dyn. Rev.* **1999**, *15*, 3–36. [CrossRef]
41. Peterson, D.W.; Eberlein, R.L. Reality check: A bridge between systems thinking and system dynamics. *Syst. Dyn. Rev.* **1994**, *10*, 159–174. [CrossRef]
42. Ford, A.; Flynn, H. Statistical screening of system dynamics models. *Syst. Dyn. Rev.* **2005**, *21*, 273–303. [CrossRef]
43. Kampmann, C.E.; Oliva, R. Loop eigenvalue elasticity analysis: Three case studies. *Syst. Dyn. Rev.* **2006**, *22*, 141–162. [CrossRef]
44. Güneralp, B. Towards coherent loop dominance analysis: Progress in eigenvalue elasticity analysis. *Syst. Dyn. Rev.* **2006**, *22*, 263–289. [CrossRef]
45. Mojtahedzadeh, M.; Andersen, D.; Richardson, G.P. Using Digest to implement the pathway participation method for detecting influential system structure. *Syst. Dyn. Rev.* **2004**, *20*, 1–20. [CrossRef]

46. Loops That Matter™ Overview. Available online: <https://www.iseesystems.com/resources/help/v2/Content/05b%20-LoopsThatMatter/LTMOverview.htm> (accessed on 12 September 2021).
47. Schoenberg, W.; Davidsen, P.; Eberlein, R. Understanding model behavior using the Loops that Matter method. *Syst. Dyn. Rev.* **2020**, *36*, 158–190. [[CrossRef](#)]
48. Schoenberg, W.; Hayward, J.; Eberlein, R. Improving Loops that Matter. Proceedings Systemdynamics.org. 2021. Available online: <https://proceedings.systemdynamics.org/2021/papers/P1036.pdf> (accessed on 18 October 2021).
49. Biggerstaff, M.; Cauchemez, S.; Reed, C.; Gambhir, M.; Finelli, L. Estimates of the reproduction number for seasonal, pandemic, and zoonotic influenza: A systematic review of the literature. *BMC Infect. Dis.* **2014**, *14*, 480. [[CrossRef](#)]
50. Vivion, M.; Sidi, E.A.L.; Betsch, C.; Dionne, M.; Dubé, E.; Driedger, S.M.; Gagnon, D.; Graham, J.; Greyson, D.; Hamel, D.; et al. Prebunking messaging to inoculate against COVID-19 vaccine misinformation: An effective strategy for public health. *J. Commun. Health* **2022**, *15*, 1–11. [[CrossRef](#)]
51. Salathé, M.; Khandelwal, S. Assessing Vaccination Sentiments with Online Social Media: Implications for Infectious Disease Dynamics and Control. *PLoS Comput. Biol.* **2011**, *7*, e1002199. [[CrossRef](#)] [[PubMed](#)]